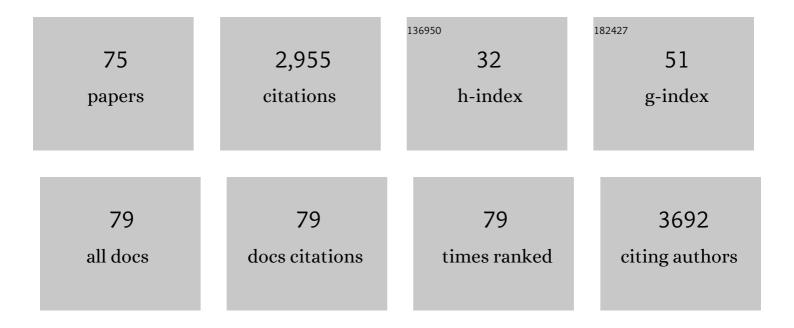
Tao He

List of Publications by Year in descending order

Source: https://exaly.com/author-pdf/639364/publications.pdf Version: 2024-02-01



#	Article	lF	CITATIONS
1	Highly efficient visible-light driven photocatalytic reduction of CO2 over g-C3N4 nanosheets/tetra(4-carboxyphenyl)porphyrin iron(III) chloride heterogeneous catalysts. Applied Catalysis B: Environmental, 2018, 221, 312-319.	20.2	186
2	In situ synthesis of ZnO/ZnTe common cation heterostructure and its visible-light photocatalytic reduction of CO2 into CH4. Applied Catalysis B: Environmental, 2015, 166-167, 345-352.	20.2	110
3	Preparation of 2D hydroxyl-rich carbon nitride nanosheets for photocatalytic reduction of CO ₂ . RSC Advances, 2015, 5, 33254-33261.	3.6	109
4	Improved visible light photocatalytic activity of titania doped with tin and nitrogen. Journal of Materials Chemistry, 2011, 21, 144-150.	6.7	106
5	Facile synthesis of Bi 2 S 3 nanoribbons for photocatalytic reduction of CO 2 into CH 3 OH. Applied Surface Science, 2017, 394, 364-370.	6.1	101
6	The doping mechanism of Cr into TiO2 and its influence on the photocatalytic performance. Physical Chemistry Chemical Physics, 2013, 15, 20037.	2.8	99
7	Preparation of CdS@CeO2 core/shell composite for photocatalytic reduction of CO2 under visible-light irradiation. Applied Surface Science, 2016, 390, 550-559.	6.1	96
8	Synergistic Effect of Charge Generation and Separation in Epitaxially Grown BiOCl/Bi ₂ S ₃ Nano-Heterostructure. ACS Applied Materials & Interfaces, 2018, 10, 15304-15313.	8.0	95
9	Synthesis of Cr-doped SrTiO3 photocatalyst and its application in visible-light-driven transformation of CO2 into CH4. Journal of CO2 Utilization, 2015, 12, 43-48.	6.8	85
10	Highly efficient visible-light driven solar-fuel production over tetra(4-carboxyphenyl)porphyrin iron(III) chloride using CdS/Bi2S3 heterostructure as photosensitizer. Applied Catalysis B: Environmental, 2018, 238, 656-663.	20.2	80
11	ZnSe/CdSe Z-scheme composites with Se vacancy for efficient photocatalytic CO2 reduction. Applied Catalysis B: Environmental, 2021, 286, 119887.	20.2	74
12	Synthesis of Indium Borate and Its Application in Photodegradation of 4-Chlorophenol. Environmental Science & Technology, 2012, 46, 2330-2336.	10.0	69
13	Self-Assembled CoS ₂ Nanocrystal Film as an Efficient Counter Electrode for Dye-Sensitized Solar Cells. Journal of Physical Chemistry C, 2014, 118, 24877-24883.	3.1	69
14	Preparation of thickness-tunable BiOCl nanosheets with high photocatalytic activity for photoreduction of CO ₂ . RSC Advances, 2015, 5, 100244-100250.	3.6	62
15	High-performance polyaniline counter electrode electropolymerized in presence of sodium dodecyl sulfate for dye-sensitized solar cells. Journal of Power Sources, 2014, 253, 300-304.	7.8	61
16	Photocatalytic Reduction of CO ₂ over Heterostructure Semiconductors into Valueâ€Added Chemicals. Chemical Record, 2016, 16, 1918-1933.	5.8	58
17	Solar-heating boosted catalytic reduction of CO2 under full-solar spectrum. Chinese Journal of Catalysis, 2020, 41, 131-139.	14.0	58
18	Synthesis of a Bi ₂ S ₃ /CeO ₂ nanocatalyst and its visible light-driven conversion of CO ₂ into CH ₃ OH and CH ₄ . Catalysis Science and Technology, 2015, 5, 5208-5215.	4.1	55

ΤΑΟ ΗΕ

#	Article	IF	CITATIONS
19	Common-cation based Z-scheme ZnS@ZnO core-shell nanostructure for efficient solar-fuel production. Applied Catalysis B: Environmental, 2018, 238, 518-524.	20.2	55
20	Crystal Facet-Dependent CO ₂ Photoreduction over Porous ZnO Nanocatalysts. ACS Applied Materials & Interfaces, 2020, 12, 56039-56048.	8.0	52
21	Preparation and characterization of SrTiO ₃ –ZnTe nanocomposites for the visible-light photoconversion of carbon dioxide to methane. RSC Advances, 2014, 4, 48411-48418.	3.6	50
22	Influence of doping anions on structure and properties of electro-polymerized polypyrrole counter electrodes for use in dye-sensitized solar cells. Journal of Power Sources, 2014, 246, 491-498.	7.8	50
23	Hollow and mesoporous ZnTe microspheres: synthesis and visible-light photocatalytic reduction of carbon dioxide into methane. RSC Advances, 2015, 5, 6186-6194.	3.6	48
24	Visible‣ight Photocatalytic Conversion of Carbon Dioxide into Methane Using Cu ₂ 0/TiO ₂ Hollow Nanospheres. Chinese Journal of Chemistry, 2015, 33, 112-118.	4.9	47
25	Study of H2SO4 concentration on properties of H2SO4 doped polyaniline counter electrodes for dye-sensitized solar cells. Journal of Power Sources, 2013, 242, 438-446.	7.8	46
26	Cu2O-tipped ZnO nanorods with enhanced photoelectrochemical performance for CO2 photoreduction. Applied Surface Science, 2018, 443, 209-216.	6.1	46
27	Enhancing TiO2 activity for CO2 photoreduction through MgO decoration. Journal of CO2 Utilization, 2020, 35, 106-114.	6.8	43
28	Facile synthesis of ZnO nanocrystals via a solid state reaction for high performance plastic dye-sensitized solar cells. Nano Research, 2012, 5, 1-10.	10.4	42
29	Optimization of charge behavior in nanoporous CuBi2O4 photocathode for photoelectrochemical reduction of CO2. Catalysis Today, 2019, 335, 388-394.	4.4	38
30	Influence of defects in porous ZnO nanoplates on CO2 photoreduction. Catalysis Today, 2019, 335, 300-305.	4.4	38
31	Modification of Ag nanoparticles on the surface of SrTiO3 particles and resultant influence on photoreduction of CO2. Applied Surface Science, 2018, 434, 717-724.	6.1	36
32	New aspects of C2 selectivity in electrochemical CO ₂ reduction over oxide-derived copper. Physical Chemistry Chemical Physics, 2020, 22, 2046-2053.	2.8	35
33	Revisiting Electrochemical Reduction of CO ₂ on Cu Electrode: Where Do We Stand about the Intermediates?. Journal of Physical Chemistry C, 2018, 122, 18528-18536.	3.1	32
34	Boosting visible-light driven solar-fuel production over g-C3N4/tetra(4-carboxyphenyl)porphyrin iron(III) chloride hybrid photocatalyst via incorporation with carbon dots. Applied Catalysis B: Environmental, 2020, 265, 118595.	20.2	31
35	An electrochemiluminescent biosensor for dopamine detection using a poly(luminol–benzidine) Tj ETQq1 1 0.	.784314 rg 2.8	gBT_/Overlock
36	Recent advances in and comprehensive consideration of the oxidation half reaction in photocatalytic $CO_{\rm CO}$ where $CO_{\rm CO}$ is a sequence of the constant of the oxidation half reaction in photocatalytic $CO_{\rm CO}$ is a sequence of the constant of	10.3	30

CO₂ conversion. Journal of Materials Chemistry A, 2021, 9, 87-110.

10.330

ΤΑΟ ΗΕ

#	Article	IF	CITATIONS
37	Fast, sensitive and selective colorimetric gold bioassay for dopamine detection. Journal of Materials Chemistry B, 2015, 3, 6019-6025.	5.8	29
38	Computational study on interactions between CO2 and (TiO2) <i>n</i> clusters at specific sites. Chinese Journal of Chemical Physics, 2019, 32, 674-686.	1.3	29
39	Low temperature fabrication of ZnO compact layer for high performance plastic dye-sensitized ZnO solar cells. Electrochimica Acta, 2012, 69, 97-101.	5.2	28
40	Terahertz Metamaterial Absorbers. Advanced Materials Technologies, 2022, 7, .	5.8	27
41	The working mechanism and performance of polypyrrole as a counter electrode for dye-sensitized solar cells. Journal of Materials Chemistry A, 2014, 2, 12805-12811.	10.3	26
42	Visible-light-driven CO ₂ photoreduction over Zn _x Cd _{1â^'x} S solid solution coupling with tetra(4-carboxyphenyl)porphyrin iron(<scp>iii</scp>) chloride. Physical Chemistry Chemical Physics, 2018, 20, 16985-16991.	2.8	25
43	Modulation of oxygen vacancy in hydrangea-like ceria via Zr doping for CO2 photoreduction. Applied Surface Science, 2018, 452, 498-506.	6.1	25
44	Recent advances in zinc chalcogenide-based nanocatalysts for photocatalytic reduction of CO ₂ . Journal of Materials Chemistry A, 2021, 9, 23364-23381.	10.3	25
45	Simple colorimetric detection of dopamine using modified silver nanoparticles. Science China Chemistry, 2016, 59, 387-393.	8.2	24
46	Study on nanoporous CuBi2O4 photocathode coated with TiO2 overlayer for photoelectrochemical CO2 reduction. Chemosphere, 2021, 264, 128508.	8.2	24
47	Influence of monomer concentration during polymerization on performance and catalytic mechanism of resultant poly(3,4-ethylenedioxythiophene) counter electrodes for dye-sensitized solar cells. Electrochimica Acta, 2015, 173, 796-803.	5.2	23
48	Unraveling the selectivity puzzle of H2 evolution over CO2 photoreduction using ZnS nanocatalysts with phase junction. Applied Catalysis B: Environmental, 2020, 274, 119115.	20.2	23
49	Ethylenediamine-functionalized CdS/tetra(4-carboxyphenyl)porphyrin iron(III) chloride hybrid system for enhanced CO2 photoreduction. Applied Surface Science, 2018, 459, 292-299.	6.1	22
50	Preparation of polypyrrole thin film counter electrode with pre-stored iodine and resultant influence on its performance. Journal of Power Sources, 2015, 274, 1076-1084.	7.8	21
51	Facile modulation of different vacancies in ZnS nanoplates for efficient solar fuel production. Journal of Materials Chemistry A, 2021, 9, 7977-7990.	10.3	21
52	Terahertz Detectors Based on Carbon Nanomaterials. Advanced Functional Materials, 2022, 32, 2107499.	14.9	19
53	ZnTe-based nanocatalysts for CO2 reduction. Current Opinion in Green and Sustainable Chemistry, 2019, 16, 7-12.	5.9	18
54	Design of a sector bowtie nano-rectenna for optical power and infrared detection. Frontiers of Physics, 2015, 10, 1.	5.0	16

ΤΑΟ ΗΕ

#	Article	IF	CITATIONS
55	Formation of Highly Stable Self-Assembled Alkyl Phosphonic Acid Monolayers for the Functionalization of Titanium Surfaces and Protein Patterning. Langmuir, 2015, 31, 140-148.	3.5	15
56	Interfacial charge kinetics of ZnO/ZnTe heterostructured nanorod arrays for CO 2 photoreduction. Electrochimica Acta, 2018, 272, 203-211.	5.2	15
57	Preparation and photolithography of self-assembled monolayers of 10-mercaptodecanylphosphonic acid on glass mediated by zirconium for protein patterning. Colloids and Surfaces B: Biointerfaces, 2013, 108, 66-71.	5.0	14
58	Visibleâ€Light Photoreduction of CO ₂ to CH ₄ over ZnTeâ€Modified TiO ₂ Coralâ€Like Nanostructures. ChemPhysChem, 2017, 18, 3203-3210.	2.1	13
59	A computational study on linear and bent adsorption of CO2 on different surfaces for its photoreduction. Catalysis Today, 2019, 335, 278-285.	4.4	13
60	Electrochemical reduction of CO ₂ : Two―or threeâ€electrode configuration. International Journal of Energy Research, 2020, 44, 548-559.	4.5	13
61	Hybrid Density Functional Theory Study on Structural and Optoelectronic Properties of ZnSe _{1–<i>x</i>} Te _{<i>x</i>} for the Photocatalytic Applications. Journal of Physical Chemistry C, 2021, 125, 16235-16245.	3.1	13
62	Photoreduction of carbon dioxide using strontium zirconate nanoparticles. Science China Materials, 2015, 58, 634-639.	6.3	12
63	Water–Gas Shift Reaction on Titania-Supported Single-Metal-Atom Catalysts: The Role of Cation (Ti) and Oxygen Vacancy. Journal of Physical Chemistry C, 2021, 125, 8620-8629.	3.1	12
64	Metamaterialsâ€Based Photoelectric Conversion: From Microwave to Optical Range. Laser and Photonics Reviews, 2022, 16, .	8.7	11
65	First-principles calculations of wurtzite ZnS1-xSex solid solutions for photocatalysis. Materials Today Communications, 2019, 21, 100672.	1.9	10
66	Visible and near-infrared dual-band photodetector based on gold–silicon metamaterial. Applied Physics Letters, 2020, 116, .	3.3	10
67	Photocatalytic materials applications for sustainable agriculture. Progress in Materials Science, 2022, 130, 100965.	32.8	10
68	Ar-plasma activated Au film with under-coordinated facet for enhanced and sustainable CO2 reduction to CO. Journal of CO2 Utilization, 2021, 54, 101776.	6.8	9
69	Controlled morphology modulation of anodic TiO2 nanotubes via changing the composition of organic electrolytes. Physical Chemistry Chemical Physics, 2014, 16, 11502.	2.8	7
70	Role of TiO ₂ coating layer on the performance of Cu ₂ O photocathode in photoelectrochemical CO ₂ reduction. Nanotechnology, 2021, 32, 395707.	2.6	7
71	Composition-tunable ZnS1–Se nanobelt solid solutions for efficient solar-fuel production. Chinese Journal of Catalysis, 2020, 41, 1663-1673.	14.0	6
72	Efficient reduction of CO2 to CO over grain boundary rich gold film reconstructed by O2 plasma treatment. Applied Catalysis A: General, 2021, 625, 118333.	4.3	6

#	Article	IF	CITATIONS
73	Controllable Modulation of Morphology and Photocatalytic Performance of ZnO Nanomaterials <i>via</i> pH Adjustment. Wuli Huaxue Xuebao/ Acta Physico - Chimica Sinica, 2016, 32, 543-550.	4.9	5
74	Synthesis and characterization of polyaniline/Zr-Co-substituted nickel ferrite (NiFe _{1.2} Zr _{0.4} Co _{0.4} O ₄) nanocomposites: their application for the photodegradation of methylene blue. Desalination and Water Treatment, 2016, 57, 12168-12177.	1.0	4
75	Low-epsilon titanium oxide antenna infrared photodetector. Optics Express, 2019, 27, 5280.	3.4	1